Desalination and Water Treatment
www.deswater.com
doi: 10.1080/19443994.2015.1035500

57 (2016) 9180–9189
April

Taylor & Francis
Taylor & Francis Group

CCD series no. 18: record low energy in closed-circuit desalination of Ocean seawater with nanoH_2O elements without ERD

Zviel Gal, Avi Efraty*

Desalitech Ltd, P.O. Box 132, Har Adar 90836, Israel, email: avi@desalitech.com (A. Efraty)

Received 5 April 2014; Accepted 2 March 2015

ABSTRACT

Experimental trials of seawater desalination under closed-circuit desalination conditions are described with a unit comprising four modules, each of four Qfx-SW-400-ES nanoH2O elements, with seawater feed in the cited (parentheses) ranges of salinity (33,801–37,197 ppm), flux (9.2–13.4 lmh), recovery (42–53%), and temperature (15.0–18.4˚C). The normalized results of this study revealed specific energies in the range of 1.453–1.775 kWh/m^3 and permeates in the range of 379–682 ppm. The lowest energy trial in the series of 1.453 kWh/m^3 with permeates of 682 ppm is observed with feed of 35,329 ppm at flux of 9.2 lmh flux and 47% recovery, and this energy is the lowest ever recorded for Ocean seawater desalination. The highest energy trial in the series of 1.775 kWh/m^3 with permeates of 548 ppm is observed with feed of 33,913 ppm at flux of 12.3 lmh and 53% recovery. In comparison with SWC6 elements in the same unit, the experimental data with the Qfx-SW-400-ES nanoH_20 elements reveals 8–12% lower energy consumption and permeates of 2–3-fold higher TDS.

Keywords: Reverse osmosis; Desalination; RO; SWRO; Closed-circuit desalination; CCD; Low energy; High recovery; Ocean seawater desalination

1. Introduction

The rapidly growing global population coupled with increased standard of living and declined availability of potable water in various parts world due to climate changes inflicted by the "*green house effect*" as well as increased contamination of ground and surface water sources have led to the growing reliance on desalinated seawater for domestic supplies. Development of membrane techniques for desalination of seawater has received considerable attention in recent years [1] with emphasis on lower energy consumption and increased salt rejection especially with regards to boron. Sea water reverse osmosis (SWRO) desalination is an energy-rich process with 35 → 65% of the desalination costs related to energy and therefore, energy saving in SWRO desalination through advance techniques and/or improved membranes is considered a principle goal aimed at meeting future SWRO desalination projections [2]. A noteworthy modern technology of low-energy SWRO is the "so-called" closed-circuit desalination (CCD) which was demonstrated [3–7] to enable high recovery with near absolute energy efficiency irrespective of the number of elements per module without need for ERD—none comprehendible features in terms the conventional plug flow desalination technologies. The nanoH_2O company has recently announced the "Quantum-Flux" line of membranes and claimed [8] major energy savings (2.49 instead of 3.47 k/Wh/m^3) when SW30HR

*Corresponding author.

elements were replaced by Qfx-SW-375-ES elements in a Cayman Islands unit of 556 m^3/d capacity-equipped PX ERD and operated with 37–40% recovery using a feed source of 34,380 ppm in the temperature range 25–29˚C.

The current study (CS) describes experimental trials with the previously reported [3,4] SWRO-CCD 4ME4 pilot; wherein E = Qfx-SW-400-ES [9] instead of the previously used SWC6 elements. The Mediterranean-derived feed used in the trials was in the salinity range 33,801–37,197 ppm and the conditions of the CCD trails were selected in the flux range 9.2–13.5 lmh, recovery range 42–53%, and temperature range 15.0–18.4˚C. The CS compares the performance of the Qfx-SW-400-ES and SWC6 elements under CCD conditions as well as of similar membranes in the context of conventional SWRO techniques. The experimental data of the CS were monitored independently by representatives of MWH Global company [10] and the Israel Aerospace Industries (IAI) [11].

2. The SWRO-CCD 4ME4(E = Qfx-SW-400-ES) Pilot

The experimental 4ME4(E = Qfx-SW-400-ES [9]) pilot used for the evaluation of the nanoH_2O elements under CCD conditions is the same as that previously reported [3,4] for the desalination of Mediterranean seawater with SWC6 membranes [12] in a site called Palmachim. The present site of the experimental pilot of the schematic design displayed in Fig. 1 is at an off-shore location of an IAI [11] facility near Tel-Aviv Israel. The feed to the pilot unit under review is supplied via a Blending Tanks System (BTS); wherein permeate and brine are mixed together to enable continuous operation with any selected seawater composition of choice. The monitored Electric Conductivity (EC) drift of the feed supplied by the BTS of different trials was found in the range of 48,809–54,600 μS/cm; however, the drift during specific trials was rather small (±0.1%) and therefore, the feed per each trial comprises a well-defined composition represented by its EC. The feed EC drift in the closed-circuit feed system under review arises from the brief intermediary steps of fast brine release which needs to be fully blended with the continuously generated permeate. Moreover, the duration of the intermediary steps and the composition of the released brine depend on the specific set points of operation selected per trial and such changes effect temporary feed EC variations. Two randomly selected feed samples were analyzed by a professional laboratory and the results displayed in Table 1 reveal rather similar compositions with average EC to salinity ratio of 1.444 (μS/cm/ppm), a value used to estimate the average feed salinity (ppm) during each of the trials. The feed stock in the BTS was created by charging the empty BTS with

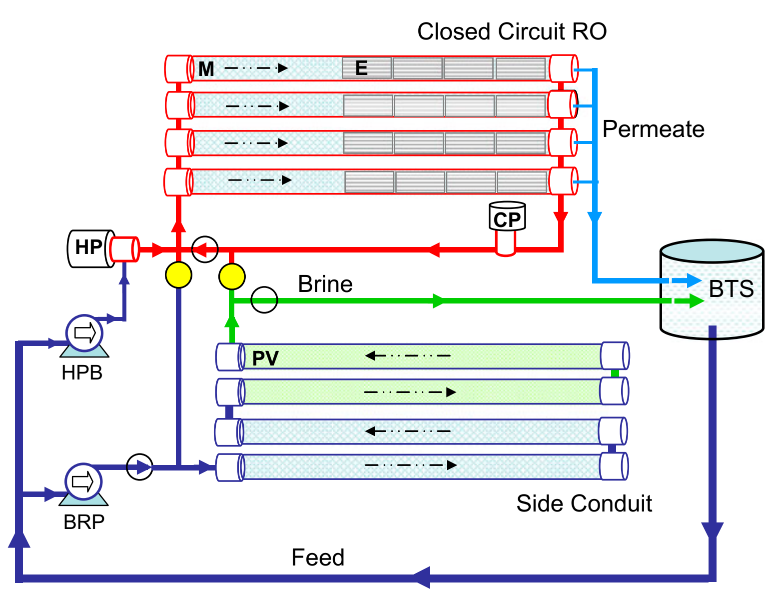

Fig. 1. The reported [3,4] schematic design of the SWRO-CCD 4ME4 pilot and its BTS for seawater feed supply during the experimental desalination trials with nanoH_2O membrane elements, showing desalination in the closed circuit (Red) and a disengaged side conduit (Blue) undergoing brine replacement by feed at near atmospheric pressure. Abbreviations: HP, high pressure pump; CP, circulation pump; HPB, high pressure booster pump; BRP, brine replacement pump; BTS, blend tanks system; M, module; E, element. PV, pressure vessel; and valves' means symbolized by circles.

Table 1
Analytical data of randomly selected SWRO-CCD feed samples from the BTS and its average EC/Salinity ratio (μS/cm/ppm) provided by the professional analytical services of Aminolab Ltd [13] Israel

Parameter	Sample 1	Sample 2	Mean
pH	7.7	7.5	7.6
Turbidity (NTU)	1	1.4	1.2
Conductivity (μs/cm)	51,700	54,600	53,150
TSD 180℃ (ppm)	36,690	36,949	36,819.5
TOC (as C) (ppm)	3	6	4.5
Cl (ppm)	19,550	16,980	18,265
Br (ppm)	53	56	54.5
B, (ppm)	4	4	4
Ca (ppm)	401	410	405.5
K (ppm)	599	715	657
Mg (ppm)	1,298	1,266	1,282
Na (ppm)	10,818	10,530	10,674
Sr (ppm)	6	6	6
μs/cm/ppm ratio	1.409	1.478	1.444

Mediterranean water (~41,000 ppm) and operating the pilot thereafter with permeates produced during the first CCD sequence diluting the original seawater feed to its ultimate salinity level. The aforementioned explains the origin of the salinity level of the stock solution in the BTS, the distinct salinity of each of the trials, and the minor salinity variation during the course of each of the trials.

3. Performance results of the SWRO-CCD 4ME4 (E = Qfx-SW-400-ES) pilot

The set points of operation and the monitored experimental results during the trials with the SWRO-CCD 4ME4 (E = Qfx-SW-400-ES) pilot using the specified Mediterranean-derived feed stock are provided in Table 2 and explained hereinafter according to the labeled rows in the table. Five different trials labeled #1 → #5 were conducted under the cited set points' conditions of fixed flow rates of HP (No. 2) and CP (No. 3) and maximum variable applied pressure (No. 4). The specified set points of operation are typical of a CCD process under fixed flow and variable pressure conditions with recovery determined independently by the set point of maximum applied pressure. The average temperature (No. 5) and its Temperature Correction Factor (No. 6) are based on the continuously monitored temperature of minor variations (±0.2℃) per trial duration of 1–2 h (No. 7). The selected time duration of 1–2 h per trial is also intended to assure small feed EC variations (<0.2%) from the average during each trial. The monitored flow rates of HP (No. 8) and CP (No. 9) are essentially the selected set points of operation and manifest the effectiveness of the *vfd*-controlled pumps through precise electromagnetic flow meters. The permeate flow rate data (No. 10) are of relatively low precision since derived from an unsophisticated domestic flow meter with volume monitoring means. The pressurized recycled concentrate bleed to the EC cell (No. 11) is manually adjusted downstream from a pressure-reducing valve. The permeation flux (No. 12) during the trials is derived from Q_{HP} (No. 8) less the bleed flow (Q_c; No. 11) by accounting for the reported [9] membrane surface area of 37 m^2, this instead the use of the directly monitored permeate flow (Q_p) which is of low precision. Incidentally, the follow balance under CCD conditions implies the relationship $Q_{HP} = Q_p$ without concentrate bleeding and $Q_{HP} = Q_p + Q_c$ with concentrate bleeding. The CCD sequential pressure variations of maximum (No. 13), minimum (No. 14), and average (No. 15) are retrieved from the continuously monitored pressure data at inlet to modules. Pressure created by HPB at inlet to HP is monitored (No. 16) and the flow-induced pressure losses along modules (Δp; No. 17) is a calculated value derived from the average cross-flow according to the expression $\Delta p(\text{bar}) = (7.2/1{,}000) \times 4 \times [(Q_{HP} + 2Q_{CP})/8]^{1.7}$ which yields near equivalent results to those predicted by the nanoH_2O design program. The average feed EC (No. 18) and concentration (No. 19) as well as the maximum EC of recycled concentrates (No. 20) and of brine concentration (No. 21) are derived from the continuously monitored EC data with translation to concentration (ppm) by means of the average conversion factor 1.444 (μS/cm/ppm) cited in Table 1. Average EC (No. 22) and concentration (No. 23) of permeates originate from analytical data of representative samples (Table 3), one per each trial collected at the average applied pressure of the selected sequence. Monitored energy consumption of HP (No. 24), CP (No. 25), HPB (No. 26) and BRP (No. 27) are metered separately with RO energy (No. 28) derived only from pumps HP + CP + HPB. The total energy consumption of the pilot (No. 29) is the sum of all the listed pumps and does not take into account the energy consumption for light, control board, and compressor. The efficiencies of HP (No. 30), CP (No. 31), and HPB (No. 32) are derived from the appropriate data of flow, pressure, and energy in Table 1. Module recovery (No. 33) is expressed by $Q_{HP}/(Q_{HP} + Q_{CP}) \times 100$, volumetric recovery (No. 34) by $\Sigma V_p/\Sigma V_f \times 100$ of total monitored permeate and feed volumes per trial, and EC recovery (No. 35) by $[\Delta EC_{(\text{Brine-feed})}/EC_{\text{Brine}}] \times 100$.

The Summary section in Table 1 covers the principle results of the trials in reference to RO specific

Table 2
Experimental results and conditions during the SWRO-CCD 4ME4 (E Qfx-SW-400-ES) pilot trials with Mediterranean-derived feed stock of cited salinity per trial

	SET POINTS of operation					
1	Trial number	#1	#2	#3	#4	#5
2	HP flow rate (m^3/h)	7.60	7.60	7.60	5.70	8.30
3	CP low rate (m^3/h)	30.60	30.60	30.60	22.80	33.20
4	Maximum applied pressure (bar)	59.0	67.0	59.0	59.0	58.0
	Experimental data					
5	Average temperature (°C)	17.0	18.4	15.0	15.9	16.8
6	Temperature correction factor	1.272	1.218	1.354	1.316	1.280
7	Duration of experiments (h)	2.00	2.00	1.00	1.00	1.00
8	HP flow Rate (m3/h)	7.62	7.55	7.52	5.69	8.22
9	CP flow Rate (m3/h)	30.36	30.50	29.96	22.64	32.54
10	Permeate flow rate (m3/h)	7.28	7.50	7.35	5.78	8.28
11	Concentrate bleed to EC cell (m3/h)	0.20	0.20	0.20	0.20	0.20
12	Flux	12.5	12.3	12.3	9.2	13.5
13	Maximum applied pressure (bar)	60.5	68.2	59.2	60.1	58.2
14	Minimum applied pressure (bar)	36.5	34.5	37.8	34.2	35.2
15	Average applied pressure (bar)	48.5	51.4	48.5	47.2	46.7
16	HP inlet pressure (bar)	0.7	0.7	0.7	0.7	0.7
17	Module Δp from flow data (bar)	1.10	1.11	1.08	0.67	1.24
18	Average feed EC (μS/cm)	53,000	50,000	52,500	51,500	49,500
19	Average feed TDS (ppm)	36,704	34,626	36,357	35,665	34,280
20	Maximum EC recycled concentrates (μS/cm)	94,090	104,320	94,592	98,304	91,776
21	Brine ppm	65,159	72,244	65,507	68,078	63,557
22	Average permeate analysis (μS/cm)	849	918	673	1,052	720
23	Average permeate analysis (ppm)	408	450	280	518	315
24	High pressure pump (HP) (kWh)	24.7	26.5	12.0	8.9	12.8
25	Circulation pump (CP) (kWh)	4.2	4.2	2.2	1.1	2.5
26	High pressure booster pump (HPB) (kWh)	1.1	1.1	0.5	0.5	0.5
27	Brine replacement pump (BRP) (kWh)	2.0	1.4	1.1	0.7	1.0
28	RO energy consumption	30.0	31.8	14.7	10.5	15.8
29	Total energy Consumption including BRP	32.0	33.2	15.8	11.2	16.8
30	HP pump efficiency (%)	81.9	80.2	83.2	82.5	82.1
31	CP pump efficiency (%)	44.3	44.8	40.8	38.3	45.0
32	HP booster pump efficiency (%)	26.9	26.7	29.2	22.1	32.0
33	Module recovery (%)	20.1	19.8	20.1	20.1	20.2
34	Recovery (Volumetric data)	45.0	53.0	42.0	47.0	47.0
35	Recovery (EC data)	43.7	52.1	44.5	47.6	46.1
	Summary					
36	RO specific energy (kWh/m3)	2.022	2.163	2.008	1.913	1.970
37	Normalized RO specific energy (kWh/m3)	1.589	1.775	1.483	1.453	1.539
38	Total energy (RO + CP) (kWh/m3)	2.156	2.259	2.158	2.040	2.095
39	Normalized total energy (RO+BRP) (kWh/m3)	1.695	1.854	1.594	1.550	1.637
40	Normalized TDS of permeates (ppm)	519	548	379	682	403
41	Salt rejection (%)	98.89	98.70	99.23	98.55	99.08

energy (SE_{RO}), both uncorrected (No. 36) and temperature corrected (No. 37) to 25°C. RO specific energy is derived from the expression ΣkWh(HP + CP + HPB)/Σm^3(HP less bleeding); wherein the cumulative monitored period is the entire trial. Both cumulative energy consumption of pumps and cumulative volume of permeates are monitored experimental parameters and therefore, the calculated term SE_{RO} is expected to meet of high precision. The SE_{RO} term makes no reference to BRP since this pump in not part of the pressurized section of the CCD process and does not contribute even to the pressurizing energy of the side conduit before engagement. The power (P, kW) for HP is defined by Eq. (1) and for CP by Eq. (2) with RO specific energy

Table 3
Analytical data of average permeate representative samples received during the SWRO-CCD 4ME4 (*E* = Qfx-SW-400-ES) pilot desalination trials with Mediterranean water-derived feed—Analytical services provided by Aminolab Ltd, Israel

Analysis of average permeate samples					
Item	Trial-#1	Trial-#2	Trial-#3	Trial-#4	Trial-#5
PH	6.3	6.4	6.6	6.6	6.6
Turbidity (NTU)	1.9	3.5	1.4	1.6	1.4
Conductivity (µs/cm)	849	918	673	1,052	720
TDS 180˚C (ppm)	408	450	280	518	315
TOC (as C) (ppm)	0.6	<0.5	≤0.5	1	0.7
Cl (ppm)	250	268	187	286	199
Br (ppm)	0.9	0.9	<1	<1	<1
B (ppm)	2	2	2	2	2
Ca (ppm)	0.5	1	0.4	0.5	0.3
K (ppm)	10	11	7	7	8
Mg (ppm)	1	1	1	2	1
Na (ppm)	150	163	114	177	119
Sr (ppm)	0.01	0.01	0.01	0.01	0.01

of the entire process expressed by Eq. (3); wherein the respective Q terms stand for flow rates (m^3/h), f terms for efficiency factor of pumps, p_{av} (bar) for average applied pressure by HP during CCD, and Δp for the fixed flow induced pressure drop along the pressure vessels. Replacement of brine in the decompressed side conduit by fresh feed can take place also by gravity from clean seawater feed received at the top a Multi-Media system in which case this recharge process becomes part of the pretreatment. The BRP pump in the pilot (Fig. 1) operates intermittently only after the side conduit with brine become decompressed and the process is stopped when the replaced volume matches the intrinsic volume of the closed circuit and this implies that BRP is not associated with the compression and/or decompression steps of the side conduit during the CCD process.

$$P_{HP} = Q_{HP} \times p_{av}/36/f_{HP} \quad (1)$$

$$P_{CP} = Q_{CP} \times \Delta p/36/f_{CP} \quad (2)$$

$$SE_{RO} = p_{av}/36/f_{HP} + (Q_{CP}/Q_{HP}) \times \Delta p/36/f_{CP} \quad (3)$$

The TDS of permeate is defined from the salt diffusion expression Eq. (4); wherein, B stands for the salt diffusion coefficient of the membrane; Cf for the feed concentration at inlet to modules; TCF for a temperature correction factor; μ for the flux; and pf for the average concentration polarization factor defined by Eq. (5) with a typical membrane coefficient (k) and an average element recovery ratio term Y_a defined by Eq. (6) for a module with n elements of Y recovery. SWRO-CCD is a consecutive sequential batch process performed under fixed flow and variable pressure conditions with a sequential change of module inlet concentration between a minimum and a maximum. In simple terms, in a specific CCD trial of fixed B, pf, TCF, and μ, the only sequential variations minimum → maximum will take with regards to C_f at inlets to modules and this will imply according to Eq. (4) sequential permeate variations (C_p) of minimum → maximum with an average permeate TDS and compositions per sequence. Average permeates samples, one per each trial, were collected and analyzed professionally, and the resulting analytical data is summarized in Table 3. The normalized average permeate TDS terms in Table 2 (No. 40) are of the TCF analyzed permeate samples in Table 3. The term percent salt rejection in the table 2 (No. 41) is expressed by Eq. (7); wherein, Cp stands for the average permeate TDS, and Cf for feed salinity.

$$C_p = B \times C_f \times pf \times (\mathrm{TCF})/\mu \quad (4)$$

$$pf = \mathrm{EXP}[\mathbf{k} \times \mathbf{Y}_a] \quad (5)$$

$$Y_a = 1 - (1 - Y)^{1/n} \quad (6)$$

$$\text{Salt Rejection}(\%) = \left(1 - C_p/C_f\right) \times 100 \quad (7)$$

4. Results and discussion

The summary of results in Table 2 is for five different feed salinities derived from Mediterranean seawater, each characterized by its unique EC and TDS as well as by the trials' conditions. The principle results of this study relate to RO specific energy, TDS of permeates, and salt rejection under the SWRO-CCD conditions of the 4ME4 pilot with Qfx-SW-400-ES elements and manifest the feed salinity, temperature, flux, and recovery of the specific trials. The RO specific energy during the trials is also a function of pumps' efficiencies which were determined in each trial independently from the appropriate experimental data of power, flow rate, and average pressure of operation.

The experimental RO energy during trials (No. 36) is defined from the energy consumption of HP + CP + HPB (No. 36) and from the TCF normalized consumption values (No. 37). The experimentally derived RO energies and their normalized values during the trials are displayed in Fig. 2 as a function of feed salinity (A), recovery (B), and flux (C).

Flux and recovery strongly influence RO energy and in the trials under review, the exceptional trials pertain to the flux of trial #4 (9.22 lmh) and to the recovery of trial #2 (53.0%). Ignoring the exceptional data of trials #2 and #4 leads to the average data of the remaining trials of 35,653 ppm feed salinity, 44.7% recovery, and 12.7 lmh flux with an average experimental RO energy of 2.000 ± 0.030 kWh/m^3 and TCF normalized energy of 1.532 ± 0.020 kWh/m^3.

The experimentally determined TDS of permeates (No. 23) and their TCF normalized values (No. 40) are displayed in Fig. 3 as a function of feed salinity (A), recovery (B), and flux (C).

According to the basic salt diffusion expression [Eq. (4)], TDS of permeates is inversely proportional to the flux and directly proportional to the feed salinity and in case of CCD, this implies the average value of the recycled concentrate at module inlets which takes into account also the recovery level of the process. Disregarding the exceptional data of flux in trial #4 (9.22 lmh) and of recovery in trial #2 (53.0%) leads to the average data of the remaining trials of 35,653 ppm feed salinity, 44.7% recovery, and 12.7 lmh flux of an

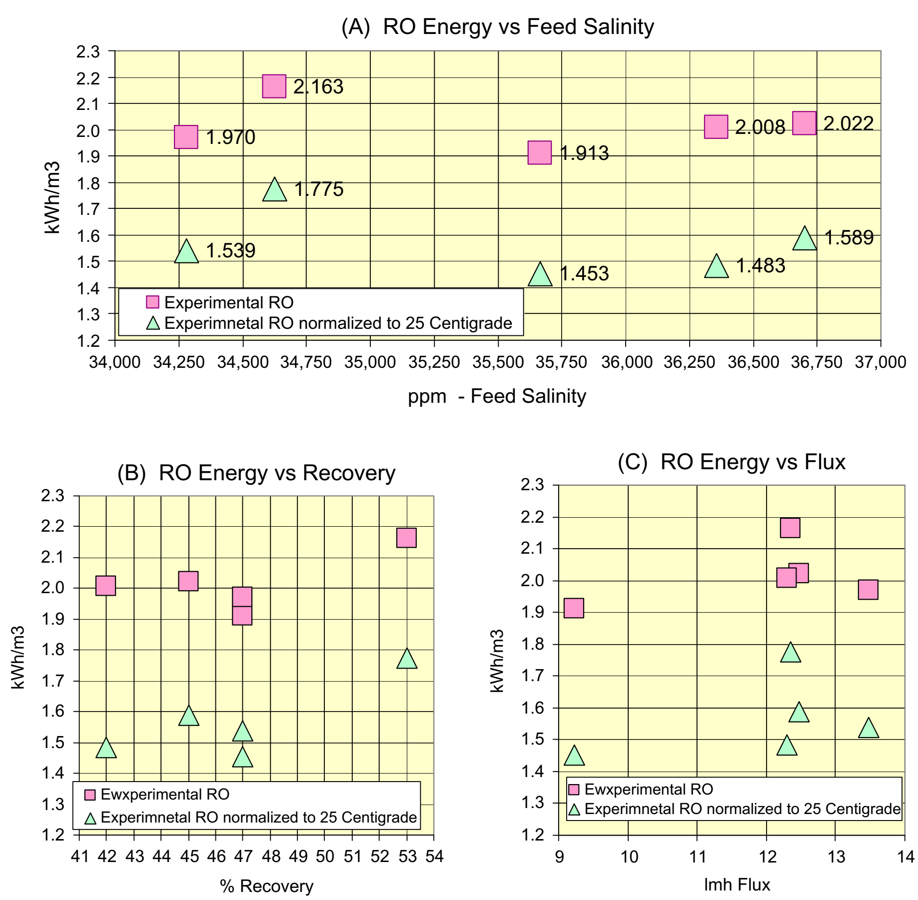

Fig. 2. Experimentally derived RO energies and their TCF normalized values as function of feed salinity (A), recovery (B), and flux (C) according to the trials' results in Table 2.

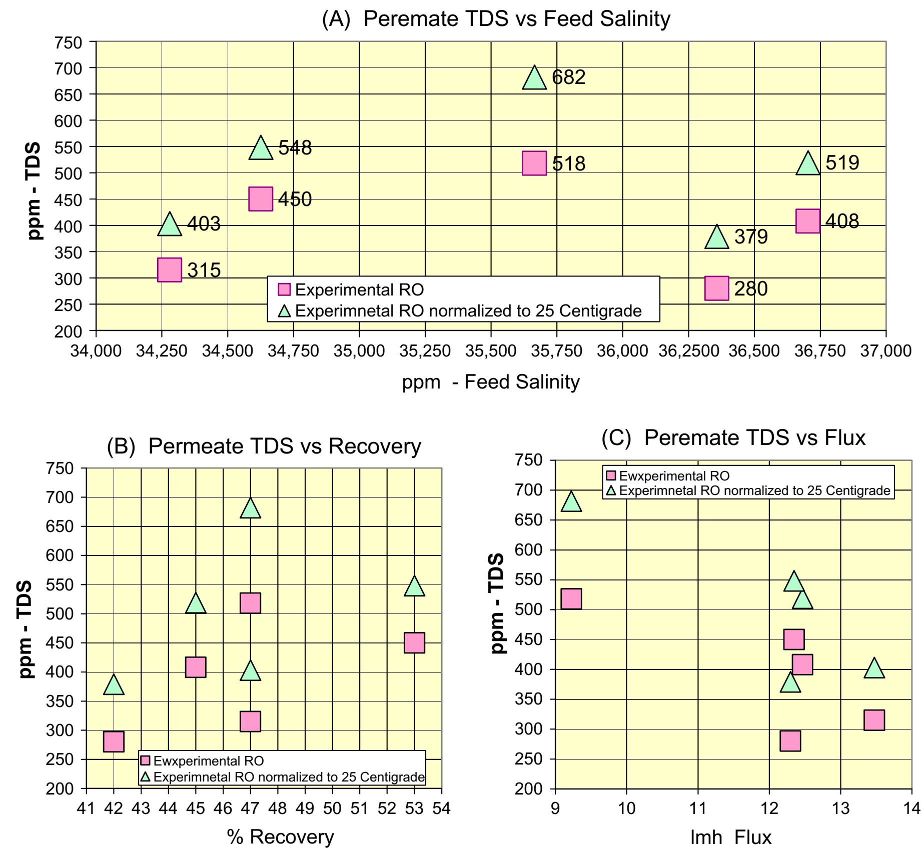

Fig. 3. Experimentally determined TDS of permeates and their TCF normalized values as function of feed salinity (A), recovery (B), and flux (C) according to the trials' results in Table 2.

average 334 ppm TDS of permeates and a 434 ppm normalized TDS TCF value.

The experimentally determined salt rejection during the trails specified in Table 2 (No. 41) is displayed in Fig. 4 as a function of feed salinity (A), recovery (B), and flux (C). Disregarding the exceptional data of flux in trial #4 (9.22 lmh) and of recovery in trial #2 (53.0%) leads to the average data for the remaining trials of 35,653 ppm feed salinity, 44.7% recovery, and 12.7 lmh flux and an average 334 ppm TDS of permeates as result of an average salt rejection of 98.88%.

5. Comparison between Qfx-SW-400-ES and SWC6 under SWRO-CCD conditions

Compared with the several hundreds of Mediterranean seawater (~41,000 ppm) trials with the SWRO-CCD 4MEn (*n* = 1–4, E = SWC6) pilot in its various configurations many of which were already reported [3, 4], only five trials were conducted to evaluate the performance the nanoH_2O Qfx-SW-400-ES membranes under CCD conditions. The five trials were conducted under different conditions according to a preconceived protocol recommended by MWH Global [10], and the results of the trials were independently collected for analysis by the representatives of this company. The summary of results obtained during the trials with the nanoH_2O elements is found in Tables 1–3, and the performance comparison between the Qfx-SW-400-ES and SWC6 membrane elements under CCD conditions is discussed next.

The Mediterranean seawater (~41,000 ppm) trials results with the same SWRO-CCD 4ME4 (E = SWC6) pilot unit operated in the indicated ranges (in parenthesis) of flux (1–16 lmh), recovery (47.5 ± 1.5%), temperature (23.2 ± 2.0°C), and HP efficiency (82.5 ± 2.0%) provided a sound performance reference for the SWC6 elements including the extrapolated performance to typical Ocean seawater (35,000 ppm) of similar feed salinity to the trials with Qfx-SW-400-ES. In order to establish common basis for comparison, the Qfx-SW-400-ES trials results of RO energy (kWh/m^3; Table 2, No. 36) and average quality permeates (ppm TDS; Table 2, No. 23) were extrapolated to manifest

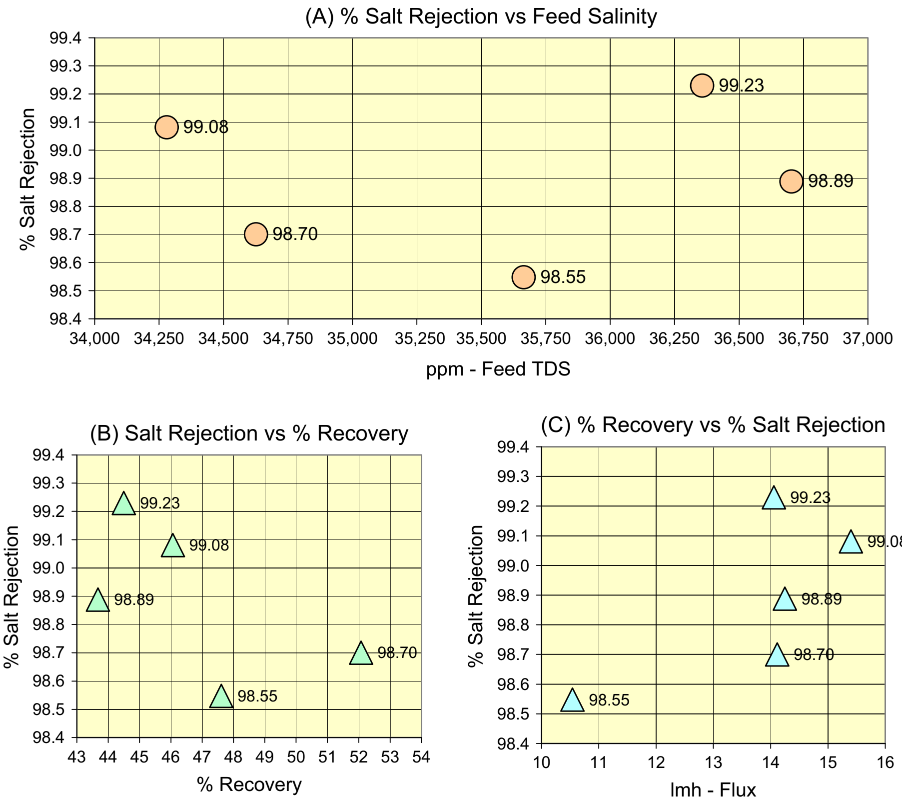

Fig. 4. Experimentally determined cumulative salts rejection as function of feed salinity (A), recovery (B), and flux (C) according to the trials' results in Table 2.

feed salinity of 35,000 ppm, recovery of 47.5%, temperature of 23.2°C, and HP efficiency of 82.5% as for the SWC6 elements, and the comparative results for both elements as function of flux are displayed in Figs. 5 and 6. The specific energy consumption of the unit with Qfx-SW-400-ES and SWC6 elements under

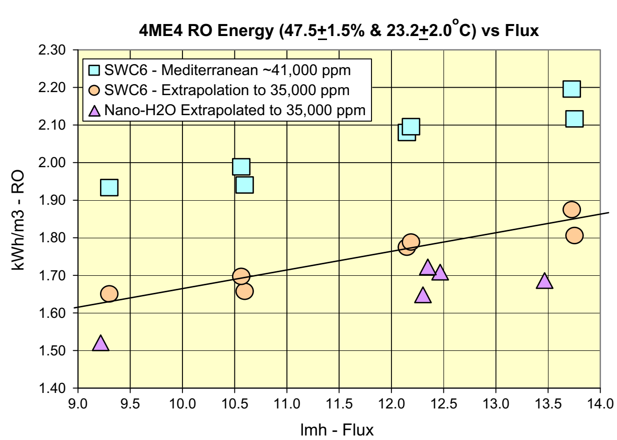

Fig. 5. Experimental RO specific energy vs. flux for SWC6 with Mediterranean seawater under CCD conditions, extrapolated values for ocean seawater, and extrapolated values for Qfx-SW-400-ES with feed of 35,000 ppm under equivalent condition.

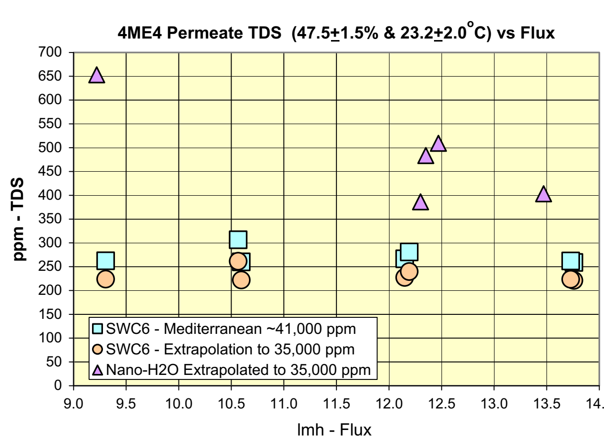

Fig. 6. Experimental TDS of permeates vs. flux for SWC6 with Mediterranean seawater under CCD conditions, showing extrapolated values for ocean seawater, and normalized experimental data under equivalent conditions for the Qfx-SW-400-ES elements.

Table 4
Overview comparison between the SWRO-CCD results of the CS and reported [8] data of conventional SWRO-PX with respect to energy consumption and quality of permeate as function of feed salinity, flux, recovery (REC), and temperature (TEMP) for different membrane elements

Technology & membranes		Feed	Flux	REC	SE	TDS	TEMP	Ref
Method	Element	(ppm)	(lmh)	(%)	(kWh/m3)	(ppm)	(°C)	
SWRO-PX	SW30HR	34,380	16.4	37.0	3.47	120	25–29	11
SWRO-PX	Qfx-SW-365-ES	31,445	17.3	40.0	2.49	263	25–29	11
SWR-CCD	Qfx-SW-400-ES	35,000	14.0	47.5	1.69	450	23.2	CS
SWR-CCD	Qfx-SW-400-ES	35,000	14.0	45.0	1.50	481	27.0	CS
SWR-CCD	SWC6	35,000	14.0	47.5	1.86	225	23.2	3&4
SWR-CCD	SWC6	35,000	14.0	45.0	1.65	241	27.0	CS

near equivalent conditions of feed salinity, recovery, temperature, and efficiency of HP pump displayed in Fig. 5 as a function of flux reveals consistently lower (9–12%) specific energy values for the former. The same comparative data presentation with respect to the average TDS of permeates displayed in Fig. 6 reveals 2–3-fold greater TDS of permeates for Qfx-SW-400-ES compared with SWC6. The theory expected trends of increased RO energy with flux in Fig. 5 and of increased TDS of permeates with declined flux in Fig. 6 rule out the presence of esoteric data and supports the trustworthiness of the conclusions reached on the basis of the study under review. The trends revealed in Figs. 5 and 6 are consistent with the assessed coefficients of the Qfx-SW-400-ES (A = 2.018 lmh/bar and B = 0.117 lmh) and SWC6 (1.75 lmh/bar and B = 0.1018 lmh) elements from their test conditions data. The higher A and B coefficients for Qfx-SW-400-ES compared with SWC6 imply the lower average applied pressure and salt rejection at the same recovery for the former elements under CCD conditions of fixed flow (fixed flux) and variable applied pressure as is manifested by the compared experimental results.

Translation of the aforementioned results into practice implies that the SWRO-CCD desalination of typical ocean seawater (35,000 ppm) with 47.5% recovery under flux of 12.7 lmh at 23.2°C requires RO energy of 1.68 ± 0.4 kWh/m^3 with Qfx-SW-400-ES and 1.76 ± 0.03 kWh/m^3 with SWC6 according to Fig. 5 with respective permeates quality of ~450 ppm and ~230 ppm according to Fig. 6.

6. Performance comparison of conventional SWRO and SWRO-CCD

A case study of a conventional SWRO plant (556 m^3/d) in the Cayman Islands comprising a positive displacement pump and an advanced PX ERD system with a booster pump for Ocean feed from a seashore well describes the performance changes incurred by the replacement of the original SW30HR elements with the nanoH$_2$O Qfrx-SW-365-ES elements. The selected data concerning feed salinity, recovery, energy, TDS of permeates, and temperature from this document are provided in Table 4 and compared with the relevant performance data of the SWRO-CCD technology with the Qfx-SW-400-ES and SWC6 elements under similar conditions. The overview comparison demonstrates the high energy and high salt rejection performance of the SW30HR membrane elements compared with the low energy and low salt rejection performance of the Qfx-SW-365-ES membrane with the conventional SWRO-PX techniques. The results in Table 4 also demonstrate the exceptionally low desalination energy enabled by the SWRO-CCD technology compared with the conventional SWRO-PX techniques. The Qfx-SW-400-ES element performance in the context of SWRO-CCD yields the lowest energy consumption term (1.50 kWh/m^3) in Table 4, much below the cited [8] value for Qfx-SW-365-ES with SWRO-PX (2.49 kWh/m^3) and/or from the reported value (2.46 kWh/m^3) [14] for the Ocean SWRO-PX plant in Perth Australia. The low-energy characteristic of the SWRO-CCD technology is also evident for the SWC6 element of much higher salt rejection compared with that of the Qfx-SW-400-ES element.

7. Summary and conclusions

Desalination of Mediterranean seawater-derived feed of 33,801–37,197 ppm salinity using the SWRO-CCD 4ME4 (E = Qfx-SW-400-ES) pilot with nanoH$_2$O elements in the flux range 9.2–13.4 lmh, recovery range 42–53%, and temperature range 15.0–18.4°C revealed normalized (25°C) RO energies of 1.453–1.775 kWh/m^3

and permeates of 379–682 ppm TDS with exact values depending on the specific conditions in each of the five trials. The lowest energy trial of 1.453 kWh/m^3 with 682 ppm normalized TDS value of average permeate arises from 35,329 ppm feed salinity, 9.2 lmh flux, and 47% recovery and demonstrates a record low energy never encountered anywhere else before for Ocean seawater desalination. The highest energy trial of 1.775 kWh/m^3 with 548 ppm normalized TDS value of average permeate arises from 33,913 ppm feed salinity, 12.3 lmh flux, and 53% recovery and demonstrates high recovery of low energy never encountered before.

In order to allow for comparison with previous results (in parenthesis) by the same pilot with SWC6 elements, the Qfx-SW-400-ES trials results were extrapolated to the near equivalent conditions of the SWC6 trials (35,000 ppm feed salinity, 47.5% recovery, 23.2˚C temperature, and 82.5% efficiency of pressurizing pump) and the comparative energy results as function of flux are found as followed: 9.22 lmh–1.521 (1.68 ± 0.01) kWh/m^3; 12.30 lmh–1.648 (1.86 ± 0.01) kWh/m^3; 12.35 lmh–1.722 (1.87 ± 0.01) kWh/m^3; 14.47 lmh–1.709 (1.88 ± 0.01) kWh/m^3; and 13.47 lmh–1.686 (1.83 ± 0.01) kWh/m^3. The TDS of permeates as function of flux for Qfx-SW-400-ES and SWC6 (in parenthesis) under the same cited near equivalent conditions are found as follows: 9.22 lmh–652 (240 ± 10) ppm; 12.30 lmh–386 (210 ± 10) ppm; 12.35 lmh–483 (210 ± 10) ppm; 12.47 lmh–509 (210 ± 10) ppm; and 13.47 lmh–403 (190 ± 10) ppm. The compared results reveal increased RO energy and salt rejection with flux for both elements as expected by theory. Furthermore, the results also show 8–12% lower energy consumption by Qfx-SW-400-ES compared with SWC6 and permeates of 2–3-fold higher TDS by the former element.

The pilot used in the study of the 4ME4 configuration comprising four pressure vessels, each of four elements, designed for 200–300 m^3/d production as function of flux. After extensive evaluation period of several years, this pilot can be viewed as a commercial demonstration unit of the new SWRO-CCD technology of low energy without ERD and high recovery irrespective of the number of elements per module, features unmatched by the conventional SWRO techniques with ERD. The record low RO energy range of 1.453–1.775 kWh/m^3 for 42–53% recovery demonstrated for Ocean seawater with the SWRO-CCD unit as compared the lowest reported energy (2.46 kWh/m^3) of a conventional SWRO-PX plant (Perth, Australia) [14] illustrates the near absolute energy efficiency achieved with the CCD technology without need of ERD.

Acknowledgments

Funds to Desalitech Ltd. by AQUAGRO FUND L.P. (Israel) and by Liberation Capital LLC (USA) are gratefully acknowledged. The data reported hereinabove were collected with the assistance of the Israel Aerospace Industry representatives under the leadership of Engineer Benaya Hoz (bhoz@iai.co.il) to whom highly indebted.

References

[1] M. Elimelech, W.A. Phillip, The future of seawater desalination: Energy, technology, and the environment, Science 333 (2011) 712–717.
[2] N. Voutchkov, Membrane seawater desalination—Overview and recent trends, IDA conference, November 2–3 2010, Huntington Beach, CA, USA.
[3] A. Efraty, R.N. Barak, Z. Gal, Closed circuit desalination—A new low energy high recovery technology without energy recovery, Desalin. Water Treat. 31 (2011) 95–101.
[4] A. Efraty, R.N. Barak, Z. Gal, Closed circuit desalination series no-2: New affordable technology for sea water desalination of low energy and high flux using short modules without need of energy recovery, Desalin. Water Treat. 42 (2012) 189–196
[5] A. Efraty, Closed circuit desalination series no-6: Conventional RO compared with the conceptually different new closed circuit desalination technology, Desalin. water treat. 41 (2012) 279–295.
[6] A. Efraty, Closed circuit desalination series no. 8: Record saving of RO energy by SWRO-CCD without need of energy recovery, Desalin. Water Treat. 52(31–33) (2014) 5717–5730.
[7] A. Efraty, CCD Series No. 11: Single module compact SWRO-CCD units of low energy and high recovery for seawater desalination including with solar panels and wind turbines, Desalin. Water Treat. 53(5) (2015) 1162–1176.
[8] Membrane Performance Contracts—NanoH2O, Available from http://www.manoh2o.com/files/mpc%20brochure%20as_web_v8-22-11.pdf.
[9] Quantum-Flux, Seawater Reverse Osmosis (RO) Element, Qfx-SW-400-ES by NanoH2O, Available from http://www.nanoh2o.com/files/qfx%sw%20400%20es%204-9-12.pfd.
[10] MWH Global, Available from http://www.mwhglo ral.com/.
[11] Israel Aerospace Industries, Available from http://iai/34640-en/Groups_EDG.aspx.
[12] Available from http://www.membranes.com/docs/8inch/SWC6.pdf.
[13] Aminolab Ltd, Israel, Available from www.amino lab.com.
[14] M.A. Sanz, R.L. Stover, Low energy consumption in the Perth Seawater Desalination Plant, IDA World Congress-Maspalomas, Gran Canaria—Spain, October 21–26, 2007 MP07.